Supporting Information

Ammonium Persulfate Assisted Synthesis of Ant-Nest-Like Hierarchical Porous Carbons Derived from Chitosan for High-Performance Supercapacitors and Zinc-Ion Hybrid Capacitors

Gui Chen,[a] Shaozhen Chen,[a] Xiaoyan Wu,[a] Caijuan Wu,[b] Yong Xiao,[a] Hanwu Dong,[a] Xiaoyuan Yu,[a] Yeru Liang,[a*] Hang Hu,[a,*] Mingtao Zheng[a,b,*]

[a] Key Laboratory for Biobased Materials and Energy of Ministry of Education/ Guangdong Provincial Engineering Technology Research Center for Optical Agriculture, College of Materials and Energy, South China Agricultural University, Guangzhou 510642, China

[b] Maoming Branch, Guangdong Laboratory of Lingnan Modern Agriculture, Maoming 525000, China

[*] Corresponding authors. E-mail: mtzheng@scau.edu.cn (M. Zheng), huhang@scau.edu.cn (H. Hu), liangyr@scau.edu.cn (Y. Liang)

Density Functional Theory Calculations

DFT calculations were conducted using the Gaussian 09 package. For conformation optimization and single energy calculations, the DFT functionals B3LYP and PBE0 were selected. These functionals account for 20% and 25% Hartree–Fock (HF) hybrid contributions, respectively. However, both B3LYP and PBE0 do not adequately describe the dispersion effects in each system. To address this, the DFT-D3 method developed by Grimme was employed to incorporate dispersion effects.

In terms of the basis set, we chose def2-svp for structure optimization and def2-tzvp for energy calculations. This choice strikes a balance between computational accuracy and efficiency.

Given the presence of both odd and even numbers of electrons in the complex system under investigation, we performed both restricted (close shell) and non-restricted (open shell) spin calculations. These calculations corresponded to singlet (S = 0) and doublet (S = 1) spin multiplicities, where M = 2S + 1."The adsorption energy (ΔEads) of metal adsorption on the surface is defined as:

$$\Delta Eads = E(complex) - E(adulterate) - E(metal)$$

where E(complex) is the energy of the optimized structure of the bonded complex, E(adulterate) is the energy of the optimized structure of the material without bonded metal ions, and E(metal) is the energy of the metal ion. According to this definition, negative adsorption energy suggests that the adsorption process is exothermic and the adsorption system is thermodynamically stable. Contrarily, a positive value corresponds to endothermic and unstable adsorption.

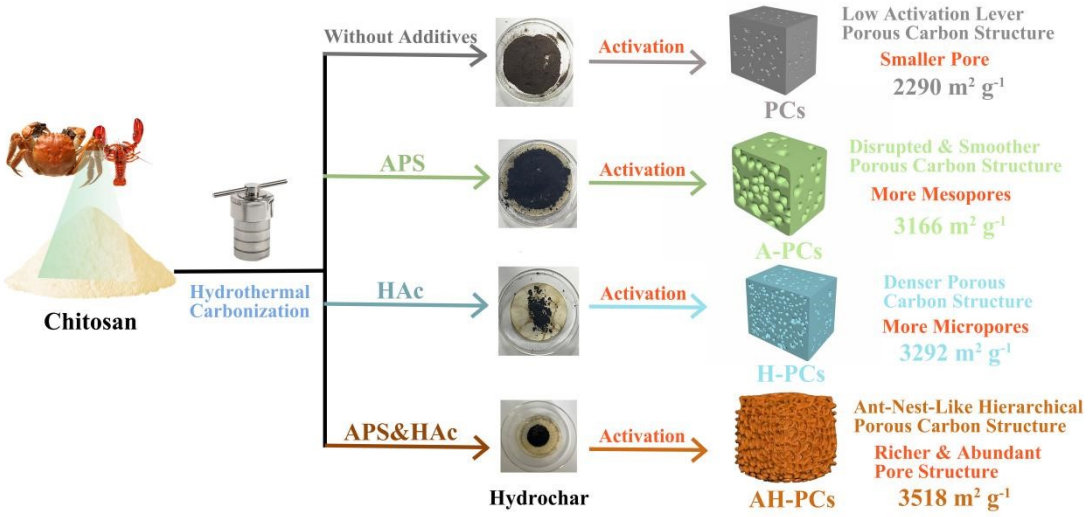

Scheme S1. Schematic of the synthesis of the chitosan-derived porous carbons.

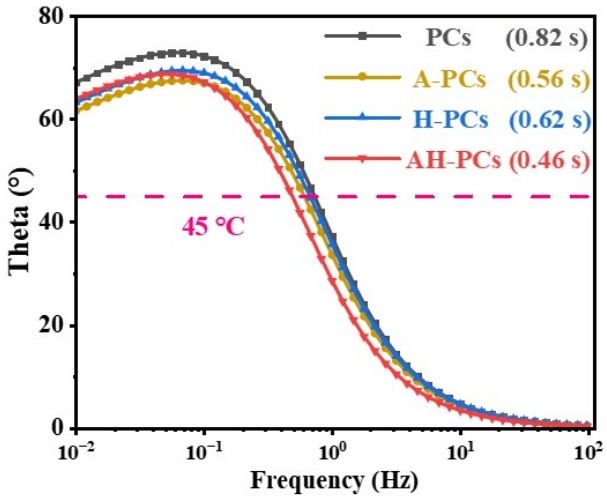

Figure S1. Bode plots.

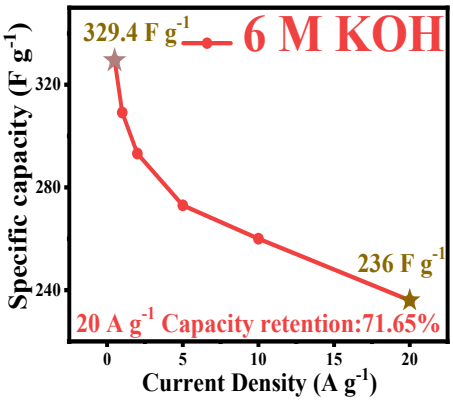

Figure S2. The specific capacitance at various current densities of AH-PCs in 6 **M** KOH Solution symmetric supercapacitors.

Table S1. The detailed parameters of specific surface area and pore volume.

Sample	S_{BET} ($m^2 g^{-1}$)	S_{mic} ($m^2 g^{-1}$)	S_{meso} ($m^2 g^{-1}$)	V_t ($cm^3 g^{-1}$)	V_{mic} ($cm^3 g^{-1}$)	V_{meso} ($cm^3 g^{-1}$)
PCs	2290	2122	168	0.93	0.82	0.11
A-PCs	3166	2122	1043	1.70	0.88	0.82
H-PCs	3292	2612	680	1.54	1.07	0.47
AH-PCs	3518	2937	581	1.57	1.22	0.35

S_{BET}: specific Brunauer-Emmett-Teller surface area;

S_{mic}: micropore surface area;

S_{meso}: mesopore surface area;

V_t: total pore volume;

V_{mic}: micropore volume;

V_{meso} : mesopore volume

Table S2. Surface element content of all samples calculated by XPS spectra.

Samples	C	N	O	% of total N1s				% of total O1s		
				N-6	N-5	N-Q	N-X	C-O	C=O	O-C=O
PCs	87.95	1.47	10.58	10.97	56.63	19.54	12.86	32.12	29.42	38.39
A-PCs	83.92	1.82	14.26	26.00	44.95	17.04	12.00	5.16	45.65	49.19
H-PCs	84.05	1.93	14.02	20.71	43.39	22.08	13.02	5.67	60.94	33.39
AH-PCs	78.51	2.74	18.75	21.82	47.61	20.75	9.82	3.67	57.66	38.67

Table S3. Comparison of BET surface area and capacitance in of AH-PCs and previously reported chitosan-derived porous carbon materials in KOH as electrolyte in three-electrode system.

Pretreatment	Activation agent	Measurement condition	BET surface area (m^2 g^{-1})	Capacitance (F g^{-1})	Ref
$Mg(CH_3COO)_2 \cdot 4H_2O$	KOH	0.5 A g^{-1} (6M KOH)	2737	226.5	S1
glutaraldehyde aqueous solution	K_2CO_3&$K_2B_4O_7 \cdot 4H_2O$	0.5 A g^{-1} (2M KOH)	3231	_____	S2
CH_3COOH& $(NH_4)_2HPO_4$	KOH	0.5 A g^{-1} (6M KOH)	3423	419.6	S3
SiO_2 nanoparticles	polytetrafluoroethylene	0.5 A g^{-1} (6M KOH)	1011	250.5	S4
glutaraldehyde aqueous solution	Zinc acetate & Tripotassium Citrate	0.5 A g^{-1} (6M KOH)	2042.3	408.9	S5
700 ℃ carbonization	KOH	0.2 A g^{-1} (6M KOH)	1129	316	S6
CH_3COOH &800 ℃ carbonization	KOH	2 mV s^{-1} (6M KOH)	2435.2	291.8	S7
phytic acid solution & dicyandiamide & glutaraldehyde	$NaNO_3$	1 A g^{-1} (6M KOH)	1010.53	231.2	S8
HNO_3&H_2SO_4& HCl &NaOH	KOH	0.2 A g^{-1} (6M KOH)	541	296	S9
$SnCl_2 \cdot 2H_2O$	selenium powder	0.1 A g^{-1} (6M KOH)	1350	260.4	S10
$(NH_4)_2S_2O_8$ & CH_3COOH	KOH	0.5 A g^{-1} (6M KOH)	3518	500	This work

Table S4. EIS parameters of PCs, A-PCs, H-PCs, and AH-PCs cathodes.

Key parameter	PCs	A-PCs	H-PCs	AH-PCs
Ohmic resistance Rs (Ω)	0.6428	0.6071	0.6314	0.5723
Charge transfer resistance Rct (Ω)	0.1253	0.1017	0.1164	0.0834

Table S5. Comparison of energy density, power density, and cycling performance of AH-PCs and previously reported biomass-derived porous carbon materials in 6 M KOH as electrolyte in a symmetric two-electrode system.

Precursor	Electrolyte	Voltage	Energy density/ Power density	Current density/ Cycle number/ Capacity retention	Ref
lignin	6M KOH	0-1V	5.1 Wh kg^{-1} at 500 W kg^{-1}	5 A g^{-1}/10000th/90.3%	S11
glucose	KOH/PVA	0-1V	10.9 Wh kg^{-1} at 125 W kg^{-1}	10 A g^{-1}/20000th/89.9%	S12
anthracite	6M KOH	0-1V	6.8 Wh kg^{-1} at 123.7 W kg^{-1}	10 A g^{-1}/10000th/98.1%	S13
Phenol & lignin phenolic	6M KOH	0-1V	3.9 Wh kg^{-1} at 125 W kg^{-1}	5 A g^{-1}/5000th/97.62%	S14
Linum usitatissimum	6M KOH	0-1V	8.16 Wh kg^{-1} at 125 W kg^{-1}	5 A g^{-1}/10000th/100%	S15
Natural apocynum	6M KOH	0-1V	7.65 Wh kg^{-1} at 500 W kg^{-1}	5 A g^{-1}/10000th/99.33%	S16
cotton stalks powder	6M KOH	0-1V	9.4Wh kg^{-1} at 249 W kg kg^{-1}	5 A g^{-1}/10000th/98%	S17
garlic peels	6M KOH	0-1V	7.42 Wh kg^{-1} at 314.33 W kg^{-1}	10 A g^{-1}/5000th/94.87%	S18
macadamia nut	6M KOH	0-1V	7.8 Wh kg^{-1} at 239 W kg^{-1}	5A g^{-1}/7000th/91.4%	S19
Chitosan	6M KOH	0-1.2V	7.86 Wh kg^{-1} at 2620 W kg^{-1}	5 A g^{-1}/10000th/97.3%	S20
Chitosan	6M KOH	0-1V	11.44 Wh kg^{-1} at 125 W kg^{-1}	10 A g^{-1} /10000th/100% 10 A g^{-1} /400000th/94.9%	This work

Table S6. Comparison of energy density, power density, and cycling performance of AH-PCs and previously reported porous carbon materials in $ZnSO_4$ as ZHICs electrode.

Cathode Material	Electrolyte	Voltage	Energy density/ Power density	Current density/ Cycle number/ Capacity retention	Ref
Yeast	2M $ZnSO_4$	0.2-1.8	94.4 Wh kg^{-1} at 80.0 W kg^{-1}	5 A·g^{-1} /7000th/100%	S21
Olive leaves	2M $ZnSO_4$	0.2-1.8	58.3Wh kg^{-1}at 20000 W kg^{-1}	10 A·g^{-1}/20000th/91%	S22
Ti_3C_2 MXene	2M $ZnSO_4$	0.1-1.3	43.89 Wh kg^{-1} at275.57 W kg^{-1}	10 A·g^{-1} /10000th/97.8%	S23
Lignin	2M $ZnSO_4$	0.2-1.8	107 Wh kg^{-1}at 86 W kg^{-1}	-	S24
ZIF-8	1M $ZnSO_4$	0.2-1.8	107.3 Wh kg^{-1} at 214.9 W kg^{-1}	10 A·g^{-1} /10000th/100%	S25
Orange peel	2M $ZnSO_4$	0.2-1.6	105.2 Wh kg^{-1} at 71.2 W kg^{-1}	10 A·g^{-1} /10000th/86.2%	S26
MOF	2M $ZnSO_4$	0.1-1.8	69 Wh kg^{-1} at 180 W kg^{-1}	1 A·g^{-1} /10000th/97.7%	S27
Furfural	2M $ZnSO_4$	0.2-1.8	97.8 Wh kg^{-1} at 80 W kg^{-1}	2 A·g^{-1} /10000th/98%	S28
Rice husks	2M $ZnSO_4$	0.1-1.8	58.6 Wh kg^{-1} at 178.6 W kg^{-1}	2 A·g^{-1} /3000th/95.8%	S29
Anthracene	3M $ZnSO_4$	0.2-1.8	109.3 Wh kg^{-1} at 33.5 W kg^{-1}	5 A·g^{-1}/10000th/ 96.2%	S30
This Work	2M $ZnSO_4$	0.2-1.8	137.6 Wh kg^{-1} at 80 W kg^{-1}	20 A·g^{-1} /20000th/ 100%	

References:

S1 D. Meng, C. Wu, Y. Hu, Y. Jing, X. Zhang, S. Mahmud, S. P. Su and J. Zhu, *J. Energy Storage*, 2022, **51**, 104341.

S2 T. Cai, Z. Yang, J. Liu, K. Xu, Y. Gao, F. Zhang, X. Yang and M. Xie, *J. Energy Storage*, 2023, **60**, 106671.

S3 F. Chen, G. Chen, P. Huang, M. Zheng, Y. Xiao, H. Hu, Y. Liang, Y. Liu and H. Dong, *J. Energy Storage*, 2023, **71**, 108180.

S4 X. Liu, X. Liu, B. Sun, H. Zhou, A. Fu, Y. Wang, Y. Guo, P. Guo and H. Li, *Carbon*, 2018, **130**, 680-691.

S5 S. Lv, L. Ma, X. Shen and H. Tong, *J. Alloy. Compd.*, 2022, **895**, 162587.

S6 Z. Lin, X. Xiang, S. Peng, X. Jiang and L. Hou, *J. Electroanal. Chem.*, 2018, **823**, 563-572.

S7 P. Hao, Z. Zhao, Y. Leng, J. Tian, Y. Sang, R. I. Boughton, C. P. Wong, H. Liu and B. Yang, *Nano Energy*, 2015, **15**, 9-23.

S8 J. Xiao, Y. Wang, T. C. Zhang, L. Ouyang and S. Yuan, *J. Power Sources*, 2022, **517**, 230727.

S9 N. Wang, G. Zhang, T. Guan, J. Wu, J. Wang and K. Li, *Acs Appl. Mater. Interfaces*, 2022, **14**, 13250-13260.

S10 Y. Lei, X. Liang, L. Yang, P. Jiang, Z. Lei, S. Wu and J. Feng, *J. Mater. Chem. A*, 2020, **8**, 4376-4385.

S11 M. Zhou, P. Wang, Y. Yu, W. Ma, Z. Cai, F. Ko, M. Li and Q. Wang, *Energy*, 2023, **278**, 127705.

S12 Y. Yang, D. Chen, W. Han, Y. Cheng, B. Sun, C. Hou, G. Zhao, D. Liu, G. Chen, J. Han and X. Zhang, *Carbon*, 2023, **205**, 1-9.

S13 G. Han, J. Jia, Y. Yao, X. Zhang, L. Yin, G. Huang, B. Xing and C. Zhang, *J. Energy Storage*, 2023, **68**, 107612.

S14 P. Li, C. Yang, D. Yi, S. Li, M. Wang, H. Wang, Y. Jin and W. Wu, *Int. J. Biol. Macromol.*, 2023, **252**, 126271.

S15 W. Tian, P. Ren, J. Wang, X. Hou, A. Sun, Y. Jin and Z. Chen, *J. Energy Storage*, 2023, **63**, 107039.

S16 Q. Tong, Q. Wang, H. Li, J. Li and W. Yang, *Adv. Sustain. Syst.*, 2023.

S17 L. Yan, A. Liu, R. Ma, C. Guo, X. Ding, P. Feng, D. Jia, M. Xu, L. Ai, N. Guo and L. Wang, *Appl. Surf. Sci.*, 2023, **615**, 156267.

S18 S. Liu, K. Dong, F. Guo, Q. Qiao, L. Xu, J. Wang, L. Kong, Y. Zhang, J. Chang and W. Yan, *J. Anal. Appl. Pyrolysis*, 2023, **173**, 106063.

S19 H. Jia, J. Sun, J. Zhu, F. Zhang, S. Li, Y. Zhang, F. Hu and X. Xie, *J. Energy Storage*, 2023, **60**, 106594.

S20 Y. Sun, D. Xu, Z. He, Z. Zhang, L. Fan and S. Wang, *J. Mater. Chem. A*, 2023, **11**, 20011-20020.

S21 Z. Dang, X. Li, Y. Li and L. Dong, *J. Colloid. Interface. Sci.*, 2023, **644**, 221-229.

S22 H. Li, P. Su, Q. Liao, Y. Liu, Y. Li, X. Niu, X. Liu and K. Wang, *Small*, 2023.

S23 Z. Li, D. Wang, Z. Sun, S. Chu and P. Chen, *Electrochim. Acta*, 2023, **455**, 142440.

S24 F. Wen, Y. Yan, S. Sun, X. Li, X. He, Q. Meng, J. Zhe Liu, X. Qiu and W. Zhang, *J. Colloid. Interface. Sci.*, 2023, **640**, 1029-1039.

S25 X. Zhu, F. Guo, Q. Yang, H. Mi, C. Yang and J. Qiu, *J. Power Sources*, 2021, **506**, 230224.

S26 J. Yu, X. Jia, J. Peng, B. Meng, Y. Wei, X. Hou, J. Zhao, N. Yang, K. Xie, D. Chu and L. Li, *Acs Appl. Energ. Mater.*, 2023, **6**, 2728-2738.

S27 X. Wang, H. Hong, S. Yang, S. Bai, R. Yang, X. Jin, C. Zhi and B. Wang, *Inorg. Chem. Front.*, 2023, **10**, 2115-2124.

S28 X. Li, J. Hu, M. Wu, C. Guo, L. Bai, J. Li, Y. Li, D. Luo, J. Duan, X. Li and Z. Li, *Carbon*, 2023, **205**, 226-235.

S29 Y. Liu, H. Tan, Z. Tan and X. Cheng, *Appl. Surf. Sci.*, 2023, **608**, 155215.

S30 F. Wei, H. Tian, P. Chen, Y. Lv and J. Huang, *Appl. Surf. Sci.*, 2023, **613**, 156021.